Applied Geochemistry 143 (2022) 105375

Contents lists available at ScienceDirect

Applied Geochemistry

journal homepage: www.elsevier.com/locate/apgeochem

Cambrian rift magmatism recorded in subvolcanic sills of the Ediacaran-Cambrian La Ciénega Formation, NW Mexico

Jesús Fernando Tapia-Trinidad [a], Arturo Joaquín Barrón-Díaz [b,*], Francisco Abraham Paz-Moreno [b], Christopher Holm-Denoma [c], James W. Hagadorn [d]

[a] Universidad de Sonora – Maestría en Ciencias-Geología, Blvd. Luis Encinas y Rosales Col. Centro, C.P.83000, Hermosillo, Sonora, Mexico
[b] Universidad de Sonora, Blvd. Luis Encinas y Rosales Col. Centro, C.P.83000, Hermosillo, Sonora, Mexico
[c] U.S. Geological Survey, Box 25046, MS 973, Denver, CO, 80225, USA
[d] Denver Museum of Nature & Science, 2001 Colorado Blvd. Denver, CO, 80205, USA

ARTICLE INFO

Editorial handling by Prof. M. Kersten

ABSTRACT

Mafic-ultramafic subvolcanic metabasalt sills intrude Ediacaran and Cambrian strata of the La Ciénega Formation of Sonora, Mexico. Sills are typically 1–7.5 m thick, with minor associated thin (~10 cm thick) intrusions. Sills are typically bed parallel with upper and/or lower tempered (quenched) borders and porphyritic textures characterized by abundant olivine and pyroxene pseudomorphs that have been transformed to clay and carbonate minerals. Metamorphic halos in adjacent dolostones and quartzites occur at the bottom and top contacts, and metabasalt sills contain carbonate veins typical of hydrothermal alteration and mobilization. Unlike surface flows of the overlying Cerro Rajón Formation, all sills in the La Ciénega Formation lack evidence of crystal settling, yet evidence for assimilation of country rocks is present. Assimilation is more typical of sills rather than flows and is diagnostic of sills in the El Arpa Formation, a stratigraphically lower unit in the succession. Actinolite-chlorite-albite metamorphic mineral paragenesis suggests low-grade greenschist facies metamorphism for these metabasaltic rocks. Although their primary mineralogy is obscured due to alteration, olivine and clinopyroxene pseudomorphs are present and their major and trace element geochemistry suggest they were derived from alkaline basaltic magmas with low (normalized) SiO_{2N} (22.7–43.1 wt%), high MgO_N (7.25–16.6 wt %), and high TiO_{2N} (4.04–6.27 wt%). Immobile trace elements suggest these sills were originally alkaline rift-related basalts with OIB-type signatures. Tectonic discrimination diagrams suggest continental rift magmatism with low geochemical evolution ratios and relatively low mantle melting rates when compared to contemporaneous rift related magmatism. Sr-Hf-Nd-Pb isotopes suggest the metabasalts originated from an Enriched Mantle I (EMI) reservoir and melting occurred during adiabatic decompression. These geochemical characteristics are remarkably similar to volcanic rocks of the Cerro Rajón Formation. The inferred magmatic composition, mantle melting rates, petrography and field relations of the La Ciénega Formation metabasalt are consistent with a low viscosity feeder system like that envisaged to have sourced volcanic rocks of the overlying Cambrian (Terreneuvian) Cerro Rajón Formation. Together, evidence from these two volcanic units is consistent with a Cambrian continental rift event close to the onset of the Sauk transgression.

1. Introduction

The ~180 m thick La Ciénega Formation of Caborca (Sonora, Mexico) is notable because its sedimentary rocks span the Ediacaran-Cambrian boundary (Stewart et al., 1984; Sour-Tovar et al., 2007; Loyd et al., 2012,a,b; Hodgin et al., 2021, Fig. 1) and because it contains mafic and ultra-mafic subvolcanic sills (Eells, 1972; Stewart et al., 1984) that have an alkaline signature typical of a continental rift setting (Centeno-García et al., 2002; Barrón-Díaz, 2013; 2019a). In western Laurentia, magmatic remnants that retain such rift signatures are rarely preserved intact because such mafic volcanics are volumetrically small and they are typically eroded by the fluvial to marginal marine environments into which they are deposited. Additionally, they are often highly altered by subsequent hydrothermal and tectonic processes (e.g.,

* Corresponding author.
E-mail addresses: ferstapia@gmail.com (J.F. Tapia-Trinidad), arturo.barron@unison.mx (A.J. Barrón-Díaz), francisco.paz@unison.mx (F.A. Paz-Moreno), cholm-denoma@usgs.gov (C. Holm-Denoma), James.Hagadorn@dmns.org (J.W. Hagadorn).

https://doi.org/10.1016/j.apgeochem.2022.105375
Received 30 December 2021; Received in revised form 26 May 2022; Accepted 13 June 2022
Available online 18 June 2022
0883-2927/

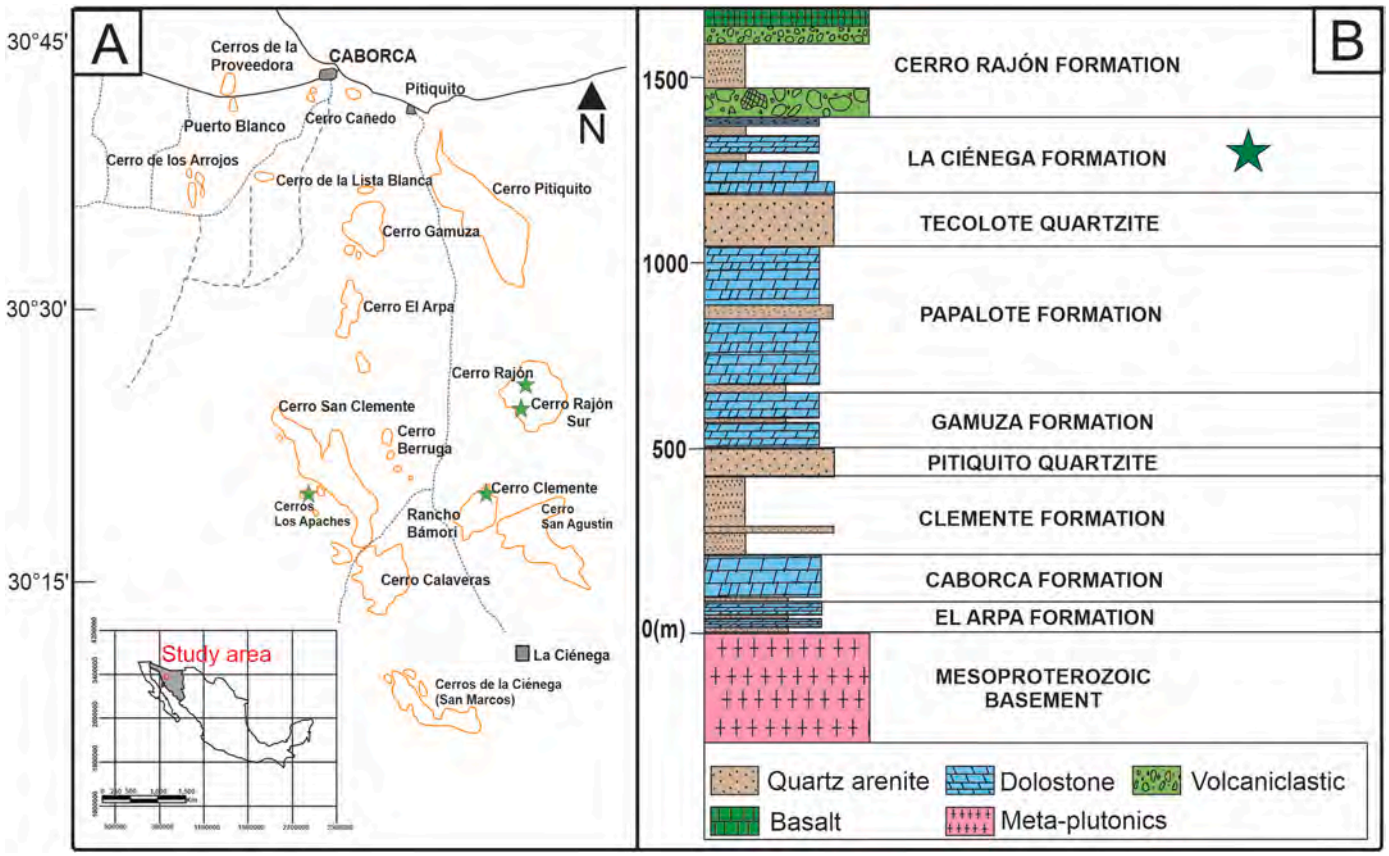

Fig. 1. A) Study area map modified from (Stewart et al., 1984). Green stars indicate the main study areas. *Inset*-regional map of Mexico and Sonora state (in gray),. The red square represents the municipality of Caborca. B) Stratigraphic column of formations reported at outcrops in the study area.

Crittenden et al., 1971; Hagadorn and Holm-Denoma, 2016; Barrón--Díaz et al., 2019c). Moreover, integrated study of such rocks is challenging (c.f. Stewart, 1972; Bond et al., 1985; Hammond, 1984; Stewart, 1991; Colpron et al., 2002; Lund et al., 2010; Yonkee et al., 2014) because dating and correlating these units is difficult, and in some cases petrogenetic and emplacement studies are lacking. With this in mind, we present the first petrogenetic and emplacement study of the La Ciénega Formation volcanic rocks. Our aim is to characterize and interpret the origin of these ultrabasic bodies, assess their relationship to volcanic rocks in the overlying Cerro Rajón Formation, and to place them into the context of other western Laurentian Ediacaran-Cambrian rift-related volcanic rocks.

2. Geological setting

The La Ciénega Formation is part of a 2.5 km-thick stratigraphic succession that spans much of late Neoproterozoic and Cambrian time and is exposed throughout Sonora (see syntheses in Stewart, 1991; Stewart et al., 2002). The first assessment of the La Ciénega Formation was by Eells (1972), who noted it was a mixed carbonate-and-clastic succession that was locally intruded by thin diabase sills. The formation was not named until two decades later, when Stewart et al. (1984) described its stratigraphy. Stewart et al. (1984) divided the formation into four predominantly carbonate to mixed carbonate-clastic units, Units 1–4, and noted that greenstones were present in Units 1 and 3. Directly dating the magmatism within La Ciénega Formation has proven challenging because these sills and their primary minerals have been altered by low-grade metamorphism (Barrón-Díaz et al., 2019c). However, maximum depositional ages of detrital zircons and $\delta^{13}C$ chemostratigraphy (see summary in Hodgin et al., 2021) indicates that these sills intruded both latest Ediacaran (Unit 1) and earliest Cambrian (Unit 3) portions of the La Ciénega Formation. Centeno-García et al. (2002) conducted the first petrological study of these sills, based on outcrops at Cerro Calaveras (Fig. 1A), and suggested that they retained geochemical and isotopic signatures of continental rift to within-plate basalts. Unfortunately, the nature of the contact between the La Ciénega Formation and the overlying Cerro Rajón Formation as well as the uppermost and basal stratigraphy of these units, varies laterally (see Barrón-Díaz et al., 2019a; 2019b), making it challenging to differentiate between the two possibly related intrusive (La Ciénega Formation) and extrusive (Cerro Rajón Formation) events.

3. Materials and methods

For this study we examined exposures of the La Ciénega Formation at Cerro Clemente, Cerro Rajón and Cerro Los Apaches (Fig. 1A). Additionally, a second stratigraphic section was described for the southern limb of Cerro Rajón. All samples from Cerro Rajón are presented together. Four reference sections from these sites are in Fig. 2, from which 37 representative hand samples of basalts were collected for petrographic and geochemical analysis. The least altered samples were selected based on field and petrographic criteria and were crushed in a jaw crusher with steel plates and pulverized in a Rescht S100 agate grinder with 12 agate balls. Major and trace element analyses were carried out at ALS laboratories in Vancouver, Canada, using the ICP-AES and ICP-MS and at the Ronald B. Gilmore X-Ray Fluorescence Laboratory at the University of Massachusetts with a using a Siemens MRS-400 multi-channel, simultaneous X-ray spectrometer (see Supplementary file 2 for details). Electron microprobe analyses were performed at the University of Arizona, Michael J Drake Laboratory with a CAMECA SX-100 (see Supplementary file 3 for details). Sr-Nd-Pb-Hf isotope analyses were performed at the Pacific Centre for Isotopic and Geochemical

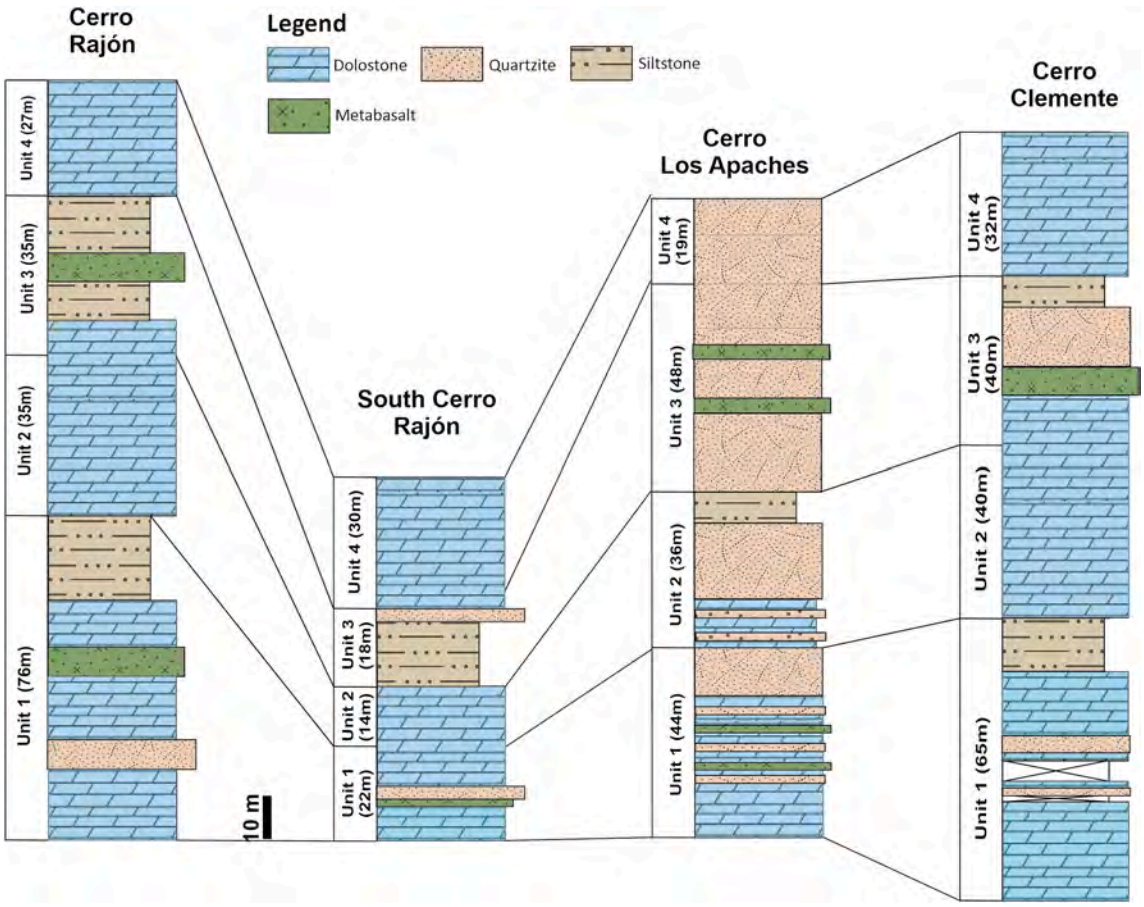

Fig. 2. Generalized stratigraphic panel diagram of the La Ciénega Formation at four of our studied localities, with metabasalt-bearing intervals indicated in green.

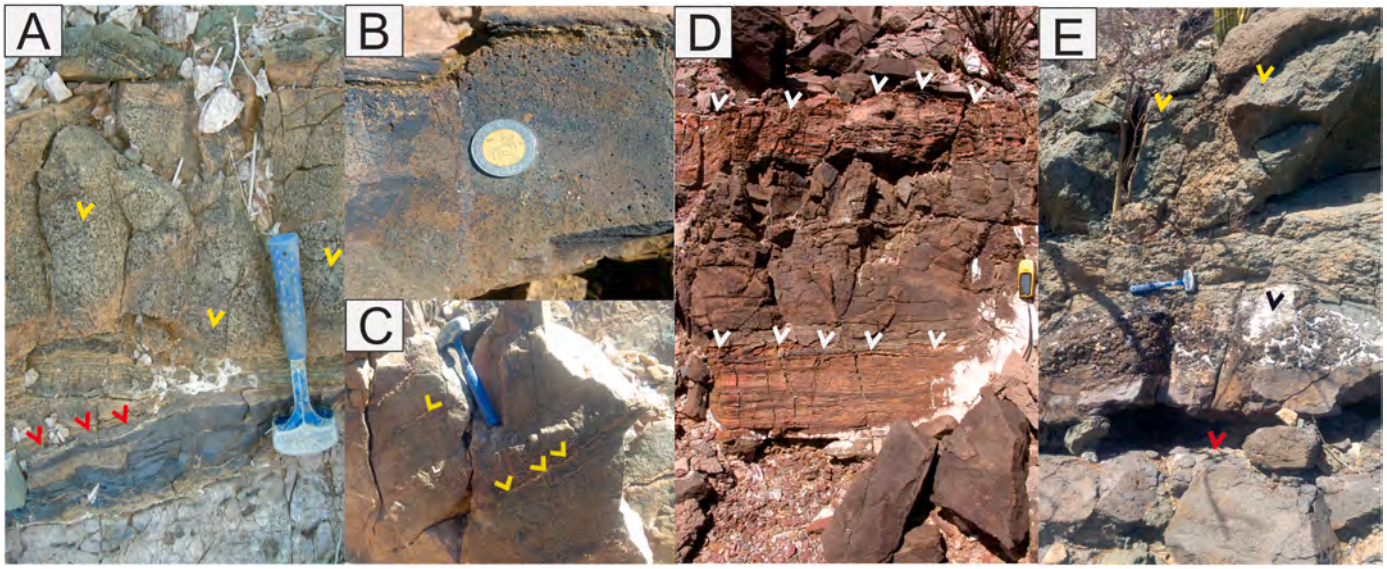

Fig. 3. Field photographs of metabasalt sills. A) Pseudovesicles that are phenocryst holes detached or lixiviated (leached) in tempered surfaces (yellow arrowheads) in La Ciénega Formation Unit 3 at Cerro Los Apaches. Tempered (quenched) border over the contact between underlying quartzite and the sill where hydrothermal alteration formed iron rich layers (red arrowheads). B) Metabasalt from El Arpa Fm at Cerro Rajón that shows tempered borders and baked quartzite atop it. Coin in photograph is 2.5 cm wide. C) Calcite and quartz veinlets (yellow arrowheads) in the El Arpa Fm metabasalt, indicative of hydrothermal activity and metamorphism. D) Metamorphic alteration halos at the upper and lower contacts between the La Ciénega Formation Unit 3 metabasalt and an intruded dolostone (white arrowheads) at Cerro Rajon. E) Metabasalt flow from Cerro Rajón Formation at Cerro Rajón, exhibiting a porphyritic vesicular texture zone (yellow arrowheads) over a volcanic scoriae base (black arrowhead) and the contact with the lower flow (red arrow); all of these characteristics are absent in the subvolcanic sills of the La Ciénega Formation. Hammer in A, C, E is 28 cm long.

Research (PCIGR), University of British Columbia using a Nu Plasma 1700 double-focusing MC-ICP-MS (Pb-Nd-Hf) and Nu TIMS (Sr), using methods described in Supplementary File 4.

4. Results & interpretations

4.1. Field relationships

Metabasalts within the La Ciénega Formation occur in Units 1 and 3, with variable numbers of sill structures as both thin (1–10 cm) and thicker, 1–7.5 m thick, bodies or composite bodies intercalated between dolostones, siltstones, and quartzites. The sills are within both Ediacaran and Cambrian strata, similar to the Cerro Rajón type section, where in Unit 1 at least three sills ranging from ~0.1 m to as much as ~7.5 m thick are intercalated within sandstones, dolostone and quartzite breccias. At this locality, the metabasaltic interval is bounded above and below by *Cloudina*-bearing dolostones. Elsewhere, in Unit 3, as many as five sills ranging from 0.1 to 1.2 m thick are intercalated with siltstones and sandy dolostones and intraformational conglomerates. At the Cerro Rajón South section (1.5 km south of the type section shown in Fig. 1A) a single 2 m thick metabasalt occurs in Unit 1, intercalated between siltstones and quartzite; this metabasalt shows abundant veins up to 1 cm thick of green minerals including actinolite and possible chlorite. At Cerro Clemente, a single ~6 m thick sill occurs in Unit 3. At Cerro Los Apaches, at least three sills, from 0.5 m to 2 m thick, occur between dolostones and quartzites. However, at Cerro Los Apaches, the succession is repeated by faults, so we are tentative in interpreting these bodies as having been emplaced in Units 1 and 3. These sills also occur in exposures of the La Ciénega Formation at Cerro San Agustín, Cerros de la Ciénega and at an unnamed exposure northwest of Cerro Calaveras (Fig. 1A).

At these localities, sills appear to be concordant with bedding. Metamorphic halos are observed in the underlying and overlying units that bound these sills. Contact metamorphism of the host sedimentary rocks extends from a few cm to more than 30 cm, as evidenced by recrystallization. These halos are more evident in dolostones, such as those that bound the second-lowest sill in Unit 3 from Cerro Rajón, where the inferred intrusion metamorphosed ~30 cm of dolostones (Fig. 3D). Such features are less evident in quartzites that bound the other sills in this succession, but contact recrystallization features are observed in thin-section microscopy.

Hydrothermal alteration is another feature of the La Ciénega Formation sills. Evidence of such alteration can be found in the Cerro Rajón South section, where in La Ciénega Formation Unit 1 exhibit abundant veins of carbonate and green minerals (e.g., actinolite and chlorite) that crosscut the metabasalts sills. Hydrothermal alteration is accentuated in sills that are in contact with dolostones, such as in the stratigraphically lower El Arpa Formation at the Cerro Rajón South locality; here a 2 m thick metabasalt intrudes the contact between an underlying dolostone and an overlying quartzite. This sill exhibits abundant carbonate veins up to 10 cm thick (Fig. 3C), suggesting that mobilization of carbonate occurred during the emplacement of these bodies. The top of this El Arpa metabasalt has baked layers of quartzite and assimilation of dolostone and quartzite clasts, and like the La Ciénega metabasalt, the crystals are uniformly distributed. In the La Ciénega Formation, this feature is best exhibited in a 0.5 m thick sill from Unit 3 in Cerro Los Apaches, where the basalt has tempered (i.e., quickly cooled, microcrystalline, non-vesicular) borders and contains abundant calcite pseudomorphs after olivine and pyroxene phenocrysts (Fig. 3A). Weathered surfaces of both the El Arpa Formation and the La Ciénega Formation sills exhibit cavities that resemble vesicles, but instead these are cavities produced by the weathering of phenocrysts (Fig. 3B). To wit, on fresh surfaces (including in thin sections) abundant phenocryst pseudomorphs occur, suggesting that these are not gas bubble vesicles. In both units, the tops of basalts are not eroded, and pyroclastic and tuffites (mixed pyroclastic-epiclastic rocks) are absent. In stark contrast, agglomerates, lapillistones, tuffs, tuffaceous conglomerates, and volcaniclastic rocks are common in the overlying Cerro Rajón Formation, as are flows with baked and loaded bases with phenocrysts and eroded to vesicular tops. Like previous authors (e.g. Eells, 1972), we did not observe any flows or extrusive volcanic rocks in the La Ciénega Formation, and there are other examples of metabasaltic sill-like bodies in underlying strata, notably in the El Arpa and Gamuza formations (Fig. 1). Collectively, these features suggest that the metabasalts within La Ciénega Formation were emplaced as shallow sills.

Table 1
Inventory of the metamorphic/alteration mineralogy and host rock fragments sorted by locality from La Ciénega and El Arpa Formation sills.

Locality	Cerro Rajón	Cerro Los Apaches	Cerro Clemente
Main metamorphic mineralogy	Cc-Act-Clay-Qz-Chl-Ab-Sph	Clay-Act-Cc-Chl-Ab-Sph	Cc-Act-Clay-Qz-Chal-Chl-Ab
Pseudomorph crystals	Px-Ol	Px-Ol	Not present
Host-rock fragments	Qz-Dol	Not present	Not present

Cc = calcite, Act = actinolite, Qz = quartz, Chl = chlorite, Ab = albite, Sph = sphene, Chal = chalcedony, Px = pyroxene, Ol = olivine, Dol = dolostone.

By examining the stratigraphic thickness of the succession between the La Ciénega and overlying Cerro Rajón Formation volcanic rocks, we can get a minimum sense of emplacement depth of these subvolcanic bodies (Figs. 1 and 2). At Cerro Rajón, the lowest La Ciénega sill (a ~0.1 m-thick basalt in Unit 1) is ~400 m below the highest extrusive volcanic in the succession (a 17 m thick basalt flow) and the highest La Ciénega sill (a ~1.2 m-thick basalt in Unit 3) is 307 m below this upper basalt flow. If one considers potential linkages between these sills and extrusive volcanics (i.e., tuffs, lappillites, agglomerates) in the succession, the thickness of strata between the lowest and uppermost La Ciénega metabasalt sills and the lowest Cerro Rajón Formation lapillite is between ~90 and ~190 m. Thus, at Cerro Rajón, if these stratigraphically superposed volcanic rocks are genetically related, La Ciénega sill emplacement could have occurred at depths between ~90 and ~400 m. Such values are comparable to those calculated from Cerro Los Apaches and Cerro Clemente and should be cautiously interpreted as minimum emplacement depth estimates, given that these values do not include corrections for compaction, erosion and other factors. Considered together, these stratigraphic relationships suggest sub-km emplacement is likely, and field relations suggest that intruded strata hadn't become well indurated. In the case of clastic rocks or sediments that contain intercalated basalts, they may still have been wet or pliable. Given these considerations, we tentatively consider the La Ciénega rocks as subvolcanic basalt bodies that were later altered to metabasalts.

4.2. Petrology

Petrographic studies were made in 21 samples from Cerro Clemente, Cerro Los Apaches and Cerro Rajón (Supplementary File 1). Low grade metamorphism and dominating porphyroblastic and granofelsic fabrics are common (Table 1). Samples from La Ciénega Formation Unit 1 and 3 at Cerro Los Apaches and El Arpa Formation at Cerro Rajón localities have pseudomorphs of primary mineralogy that are completely replaced, mostly by carbonate and clay minerals (Fig 4 A,C). Host rock fragments composed of quartz and calcite with alteration halos, and skeletal host rock fragments near the borders of the metabasalt sills occur in La Ciénega Formation Unit 3 at Cerro Rajón and in the El Arpa Formation metabasalt (Fig. 4 B,E), suggesting assimilation from country rocks.

There are three groups of metabasalt sills in the studied samples: the first group includes clay-rich metabasalt with a clay > actinolite > quartz-chalcedony > calcite > chlorite > biotite > ilmenite-magnetite paragenetic association (Fig. 4A); this alteration group is predominant at the Cerro Los Apaches locality but can also be observed in Cerro Clemente and Cerro Rajón. In addition, this alteration group shows

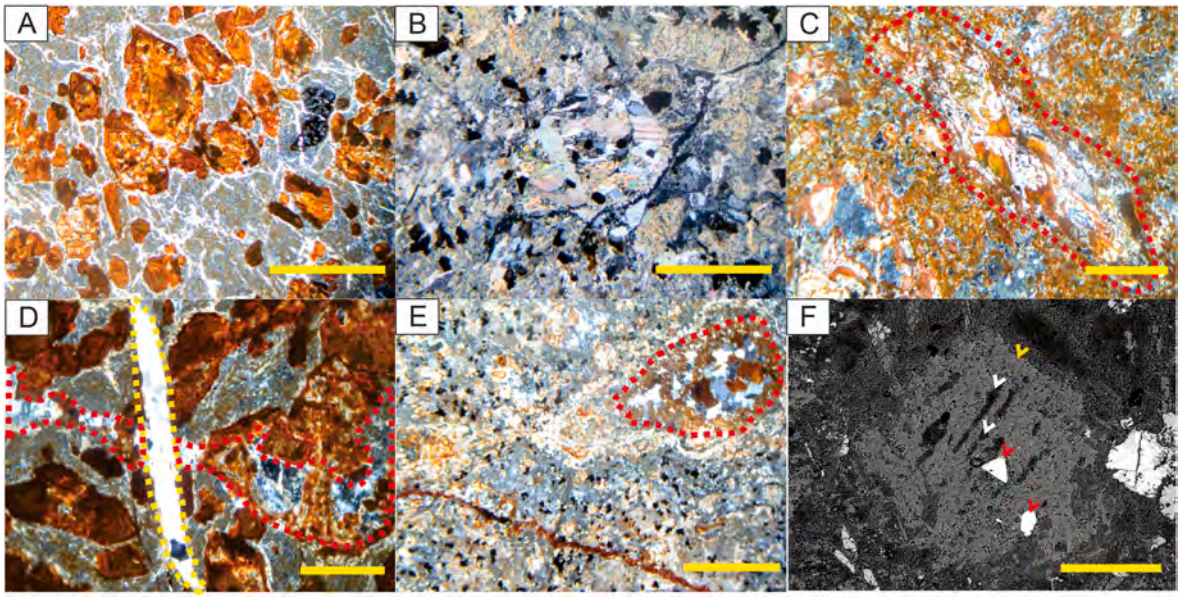

Fig. 4. Cross-polarized light photomicrographs where pseudomorphs resemble olivine and pyroxene shapes (A–E) and backscattered EMPA image (F) of La Ciénega Formation metabasalts illustrating metamorphic textures and alteration mineralogy. The porphyroblasts are mainly carbonate, chloritized biotite and amphibole that indicate low grade metamorphism. Pseudomorphs after olivine and pyroxene illustrate the primary mineralogy of these rocks and the absence of dynamo-thermal metamorphism. A) Amphibole-biotite crystals in a clay-calcite matrix (MXCR-7A-U3, La Ciénega Fm Unit 3, Cerro Rajón). B) Subhedral to polygonal calcite in a calcite-clay matrix on carbonate-rich metabasalt (MX-CR-LCU1-38m-B, La Ciénega Fm Unit 1, Cerro Rajón). C) Skeletal aggregates of calcite, chlorite and amphibole as olivine-pyroxene pseudomorphs with alteration halos (red dashed line) in a clay-calcite and quartz matrix (MX-CR-LU3-43m-C, La Ciénega Fm Unit 3, Cerro Rajón). D) Red amphibole porphyroblasts cut by a carbonate veinlet (yellow dashed line) that also cuts a silicate veinlet (red dashed line); (MXCR-7A U3, La Ciénega Fm Unit 3, Cerro Rajón) showing the timing of events. These include an initial low grade metamorphism event that created amphiboles, followed by a two-phase hydrothermal event including a silification phase followed by a carbonate phase. E) Recrystallized host rock fragments with alteration halos (red dashed line) in a carbonate-clay matrix (AB11-31, La Ciénega Fm Unit 3, Cerro Los Apaches). F) Pseudomorph after a clinopyroxene, now composed of calcite (yellow arrowhead), quartz (white arrowhead) and ilmenite (red arrowheads) aggregates (MXCR-38m-C, La Ciénega Fm Unit 1, Cerro Rajón) (EMPA Image). Scale bars are 0.25 mm in A to E and 0.20 mm in F.

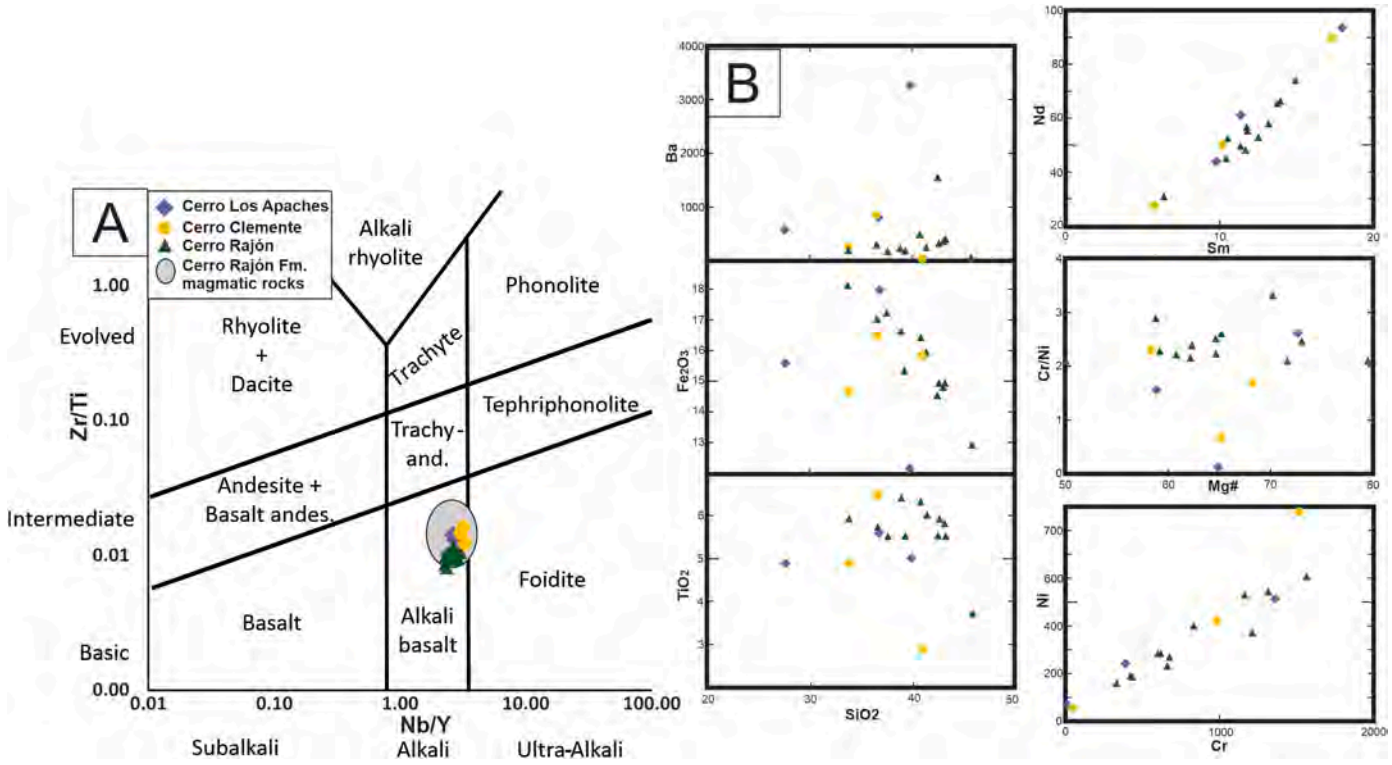

Fig. 5. A) Zr/Ti vs Nb/Y immobile trace element diagram of Pearce (1996) for volcanic rock classification. Samples from all three localities are plotted and indicate the La Ciénega bodies were originally alkali basalts. B) Harker variation diagrams for the La Ciénega sills.

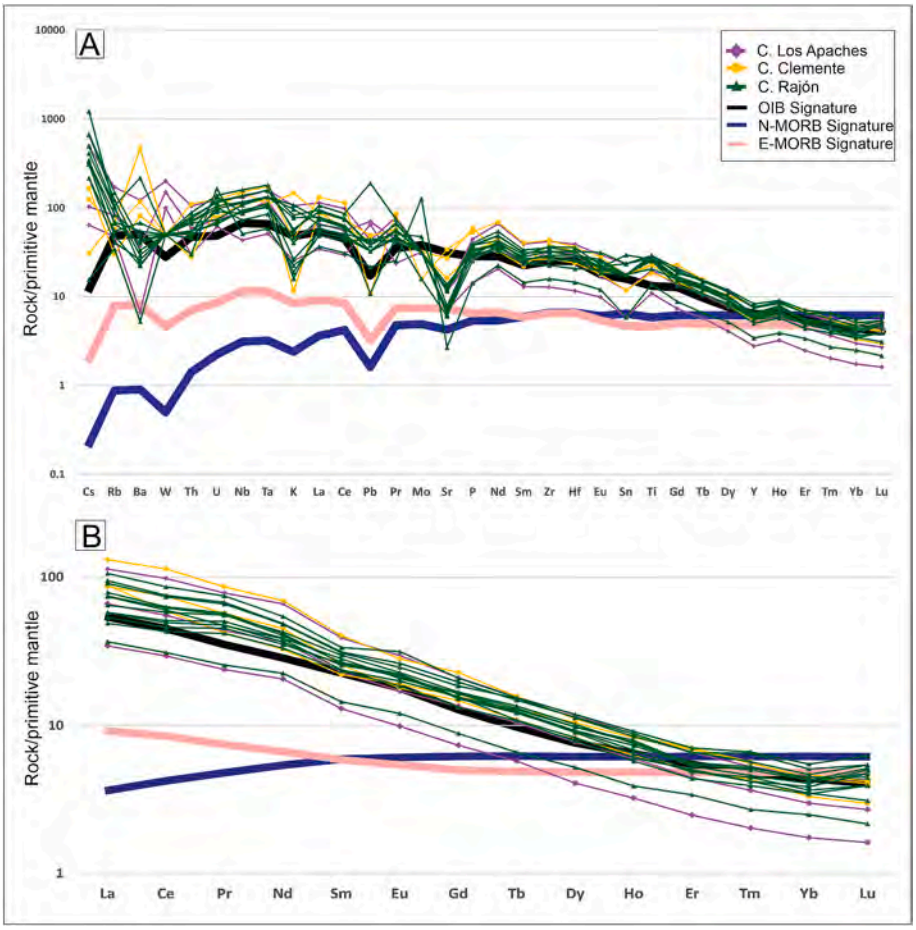

Fig. 6. A) Trace element "spider" diagram of La Ciénega Formation samples, normalized to primitive mantle (Sun & Mc.Donough, 1989) Ocean island basalt (OIB) and mid-ocean ridge basalt (MORB) values (Sun & Mc.Donough, 1989) are shown for comparison. B) REE normalized to Primitive Mantle (Sun and McDonough, 1989) of La Ciénega Formation samples. Ocean island basalt (OIB) and mid-ocean ridge basalt (N-MORB & E-MORB) values (Sun & Mc.Donough, 1989) are shown for comparison.

inferred inclusions of sandstone rock fragments composed of recrystallized quartz with alteration halos and inferred inclusions of limestone rock fragments of recrystallized calcite. These are an indication of heat alteration and assimilation caused by intrusion of sill bodies. Studied samples also contain calcite/quartz veinlets with dispersion halos, which are another indication of hydrothermal alteration. The second alteration group includes calcite-rich metabasalt sills with a calcite > clay > quartz > biotite > albite > chlorite > sphene > ilmenite-magnetite paragenetic association (Fig. 4B). This alteration group is predominant at the Cerro Rajón outcrops with minor occurrences in Cerro Clemente and Cerro Los Apaches. These rocks have carbonatization and hypogenic argillitization as their main alteration processes and contain olivine-pyroxene pseudomorphs. These pseudomorphs illustrate how was the mineral habits of the sills before alteration. The last alteration group is only observed at Cerro Rajón and includes clay and quartz-rich metabasalt sills with a clay minerals > quartz > calcite-biotite > sphene > rutile > ilmenite-magnetite paragenetic association (Fig. 4C). These rocks have a hypogenic argilitization and carbonatization with chlorite and actinolite as the main alteration processes and olivine pseudomorphs replaced by clays, carbonates and iron oxides (Fig. 4D). Metamorphic mineral assemblages of actinolite, chlorite, calcite and albite, identified through electron microprobe analysis (EMPA), suggests a greenschist facies metamorphism. All localities contain one or more alteration groups, suggesting that the alteration type could be governed by the composition of the adjacent intruded rocks and the composition of impacting hydrothermal fluid(s). All samples appear to be linked to the same greenschist facies alteration processes but with slightly different reactants.

4.3. Mineral chemistry

As a follow up to petrographic analyses, and to further determine the mineral composition and metamorphic paragenesis of the La Ciénega Formation sills, EMPA of three samples from Cerro Rajón were conducted (Supplementary File 2). Amphiboles classified as actinolite were identified in La Ciénega Formation Unit 1 from Cerro Rajón, which indicate low-grade metamorphism derived from Fe- and Mg-rich primary minerals. Chlorite from La Ciénega Formation Unit 3 at Cerro Rajón and Cerro Los Apaches was also identified. While searching for a possible datable mineral or a geothermometer, plagioclase group minerals from La Ciénega Unit 1 at Cerro Rajón were also analyzed. Results show mainly albite-oligoclase (Ab 89.6%, An 9.1%, Or 1.2%) and albite (Ab 89.4%, An 1.6%, Or 8.8%). Unfortunately, plagioclase from La Ciénega Formation metabasalts is highly altered. Consequently, geothermometers and geochronologic proxies of primary conditions are not preserved in this mineral. Nevertheless, the albitization of this plagioclase supports our field and petrologic interpretation of low grade, greenschist facies metamorphism. As previously mentioned, EMPA-determined mineral chemistry, together with the petrography results, suggest greenschist facies metamorphism for these rocks, with variable degrees of carbonate alteration. Results and calculations for the structural formulae are in Supplementary File 2.

Nomenclature

Due to the metamorphism of the La Ciénega Formation magmatic rocks, the characterization of these ultrabasic sills was made based on the classification of contact metamorphic rocks from the IUGS Subcommission on the Systematics of Metamorphic Rocks, where the

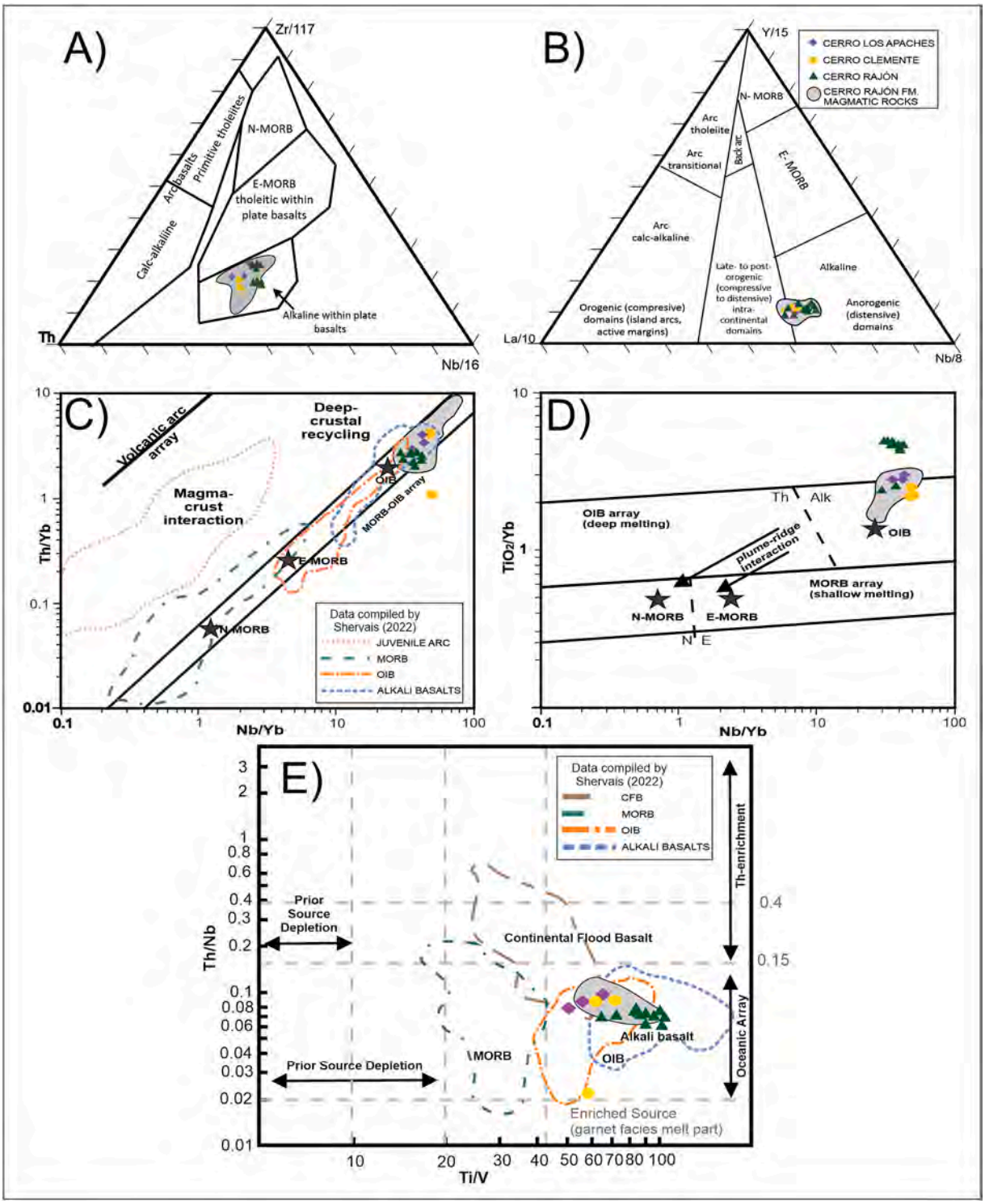

Fig. 7. Tectonic discrimination and mantle source diagrams based on immobile trace elements. A) Th–Zr–Nb basalt tectonic discrimination diagram of Wood (1980). B) La–Y–Nb basalt tectonic discrimination diagram of Cabanis and Lecolle (1989) C) Th/Yb vs Nb/Yb mantle source diagram from Pearce (2008); dashed line fields display tectonic environment data compiled by Shervais (2022). D) TiO_2/Yb vs Nb/Yb mantle source diagram from Pearce (2008). E) Ti/V vs. Th/Nb diagram with tectonic arrangement fields compiled by Shervais (2022) N-MORB (normal mid-ocean ridge basalt; E-MORB (enriched mid-ocean ridge basalt); OIB (ocean island basalt). Gray dashed lines represent Cerro Rajón Formation magmatic rock data from Barrón-Díaz (2019).

specific name proposed for these rocks is mafic ultramafic hornfels (Callegari and Pertsev, 2007). That said, we employed immobile trace element analyses to characterize the protolith using Zr/Ti vs Nb/Y concentrations (Pearce, 1996), which indicate that all the samples from La Ciénega Formation lie in the alkali-basalt field (Fig. 5A) and supports our use of the metabasalt nomenclature.

4.4. Protolith characterization

To determine the primary conditions of the metabasalt sills, major- and trace-element analyses were conducted on eighteen least-altered samples from Cerro Rajón, Cerro Los Apaches and Cerro Clemente. Samples are treated by locality rather than by unit because Unit 1 and

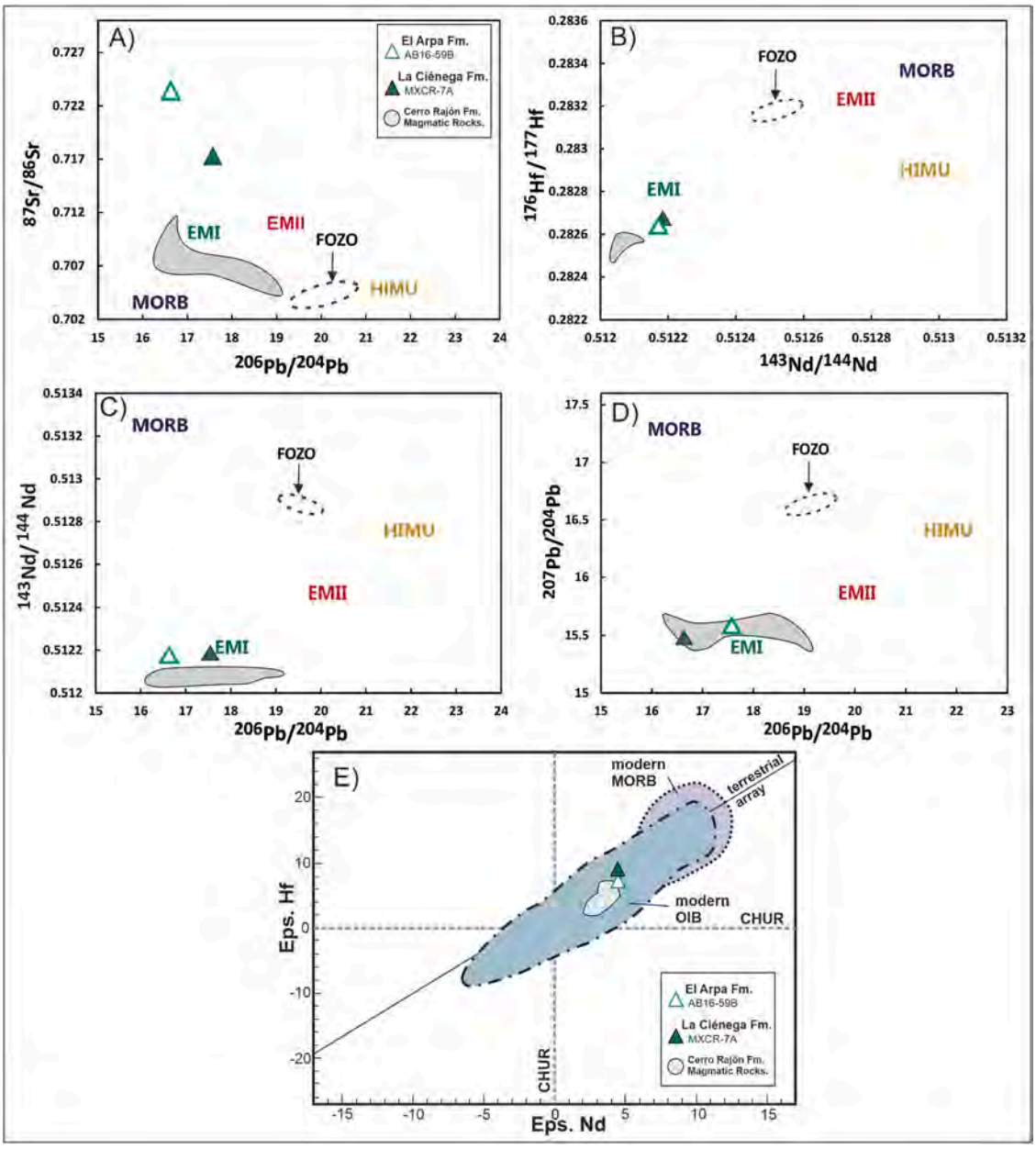

Fig. 8. Mantle reservoir source isotope diagrams of samples from La Ciénega Formation Unit 3 and the El Arpa Formation at Cerro Rajón and the Cerro Rajón Formation magmatic rocks (gray field). A) $^{87}Sr/^{86}Sr$ vs $^{206}Pb/^{204}Pb$. B) $^{176}Hf/^{177}Hf$ vs $^{143}Nd/^{144}Nd$. C) $^{143}Nd/^{144}Nd$ vs $^{206}Pb/^{204}Pb$. D) $^{207}Pb/^{204}Pb$ vs $^{206}Pb/^{204}Pb$ Similarities between these isotopic signatures suggests that volcanics in both units are related to an EMI- Enriched mantle I; EMII- Enriched mantle II; FOZO- Focused zone; HIMU- High-μ (238U/204 Pb). Mantle reservoirs and FOZO locations from Stracke et al. (2003, 2005). E) Epsilon Hf vs Epsilon Nd diagram of a sample from the La Ciénega Formation Unit 3 and El Arpa Formation at Cerro Rajón, modern MORB and OIB fields were obtained from Tappe et al. (2007); the gray field shows the Cerro Rajón Formation magmatic rocks (Barrón-Díaz, 2019).

Unit 3 sills exhibit similar geochemical characteristics. Details of major and trace element analyses are in Supplementary File 3. Major element geochemistry exhibits high TiO_2 values (4.04–6.27 wt%.), low Na_2O values (0.01–0.59 wt%) and high loss on ignition (LOI) (12.8–22.3 wt %). High LOI values suggest significant alteration of the rocks and/or the abundance of volatiles (e.g. CO_2 from carbonate) impacting the accuracy of major element concentrations. However, some trace elements, especially the high field strength elements, appear to be immobile, especially at the mineral scale as is indicated by previous analyses of volcanic clasts from the overlying Cerro Rajón Formation (Barrón-Díaz et al., 2019a). La Ciénega Formation metabasalts have high Cr (<1520 ppm) and Ni (<882 ppm) values with little variation; it is a characteristic of primary magma composition (Fig. 5B). Multi-element diagrams of La Ciénega Formation samples, normalized to primitive mantle (Sun and McDonough, 1989) show a positive hump-shaped spectrum (Fig. 6A), with positive anomalies of Nb–Ta (159–180 ppm, respectively), which is a common characteristic of ocean island basalt (OIB)-type magmatism and intraplate settings. Variable amounts of Ba (36–3270 ppm.) and negative anomalies of Sr (2.7 ppm) and Pb (10.8 ppm) were observed (Fig. 6A); these values suggest a possible crustal contamination/assimilation and/or alteration. Moreover, the La Ciénega Fm REE diagram (Fig. 6B), normalized by a PRIMA (Primitive Mantle) from Sun and McDonough (1989) shows high LREE (La = 131 ppm; Ce = 113 ppm), and very low HREE (Lu- 1.6 ppm; Yb-1.7 ppm) values and absence of Eu anomalies. The latter spectra are also related to OIB type magmatism and the absence of an Eu anomaly supports the lack of plagioclase fractionation.

This relationship is also observed in the Cerro Rajón Formation extrusive volcanics (Barrón-Díaz, 2019), where flows have ankaramitic textures and lack plagioclase.

5. Discussion

5.1. Tectonic setting characterization by trace element geochemistry

Tectonic discrimination diagrams based on relatively immobile trace elements demonstrate that the La Ciénega Formation metabasalts cluster together and mainly plot in the OIB fields or intracontinental settings with enriched mantle signatures (Fig. 7). Analyses of Th, Zr and Nb (Wood, 1980) place these rocks in an alkaline within-plate setting (Fig. 7A). This characteristic is further supported by employing a Y–La–Nb diagram (after Cabanis and Lecolle, 1989); La Ciénega Formation samples plot in the within-plate basalt and the alkaline-anorogenic domain, with few samples plotting in the late and post-orogenic intracontinental domains (Fig. 7B). Moreover, plotting the same immobile elements in a Pearce (2008) diagram supports an OIB affinity (Fig. 7C and D); here the primary condition of the magmatism is also observed (note the absence of deep crustal recycling in Fig. 7C). Similarly, Th/Yb vs Nb/Yb comparison of La Ciénega samples also plot inside the OIB and alkali basalt fields from Shervais (2022). La Ciénega Formation samples that fall outside of this field in the TiO_2/Yb vs Nb/Yb diagram from Pearce (2008; Fig. 7D), may be explained due to an enrichment in TiO_2, a primary characteristic also noted in high-TiO_2 diopsides from the overlying Cerro Rajón Formation (Barrón-Díaz et al., 2019a). The Shervais (2022) Ti/V vs Th/Nb diagram supports the placement of La Ciénega Formation rocks between the OIB and alkali basalt fields (Fig. 7E). Considered together, these characteristics suggest that the La Ciénega Formation metabasalts represent a rift-related volcanic event that developed in early Cambrian time and that a genetic correlation exists between the metabasalt sills of the La Ciénega Formation and the extrusive volcanism of the Cerro Rajón Formation.

5.2. Mantle reservoir & magmatic model

Sr-Nd-Pb-Hf isotope analyses were conducted on the La Ciénega Formation and El Arpa Formation metabasalts (Supplementary File 4) to determine their mantle reservoir affinities. Isotope initial values were recalculated to 540 Ma, which is close to the time when we hypothesize that the overlying Cerro Rajon Formation was deposited (Stewart et al., 1984; Sour-Tovar et al., 2007; Barrón-Díaz et al., 2019b). Both La Ciénega Formation and El Arpa Formation samples exhibit high initial $^{87}Sr/^{86}Sr$ values (0.7170566–0.72325), very low initial values of $^{143}Nd/^{144}Nd$ (0.51217–0.51218), $^{208}Pb/^{204}Pb$ (36.55–39.95), $^{207}Pb/^{204}Pb$ (15.46–15.57), and $^{206}Pb/^{204}Pb$ (16.63–17.57) and low initial values of $^{176}Hf/^{177}Hf$ (0.28262–0.28266). These ratios and their εNd_{540Ma} (4.53–4.73) and εHf_{540Ma} (7.22–8.52) values, are similar to those of the overlying Cerro Rajón Formation volcanic rocks (Fig. 8E), which suggests these rocks were sourced from magma of a similar isotopic reservoir.

All of these isotopic ratios suggest an enriched mantle I (EMI) source (Zindler and Hart, 1986) that may be related to hot spot interactions (Garapić et al., 2015). The EMI source is a mantle reservoir with high Sr–Rb–Mg values. The origin of this mantle reservoir is unknown, but there are multiple hypotheses about northern hemisphere EMI volcanism worth considering for our La Ciénega Fm data. For example, Kimura et al. (2016) propose that such EMI source material comes from mantle wedge peridotites that were subducted and enriched in large-ion lithophile elements (LILE) from sediments in the subducting slab, while experiencing high degrees of metasomatism by the related fluids driven out of sedimentary rocks by subduction dehydration. Other hypotheses suggest recycling of the lower continental crust (LCC; Willbold and Stracke, 2006; 2010) or delamination of the Sub Lithospheric Continental Mantle (SLCM) (Hoernle et al., 2011; Tatsumoto and Nakamura, 1991). The average estimated ages for this northern hemisphere mantle source range from ~0.5 to 1.7 Ga (Kimura et al., 2016). Regarding the association of La Ciénega magmatism with Cerro Rajón Formation volcanism, we hypothesize that the ascent mechanism may have resulted from adiabatic decompression processes. This would explain the absence of an identified magmatic chamber and the low differentiation values observed in the metabasalt sills.

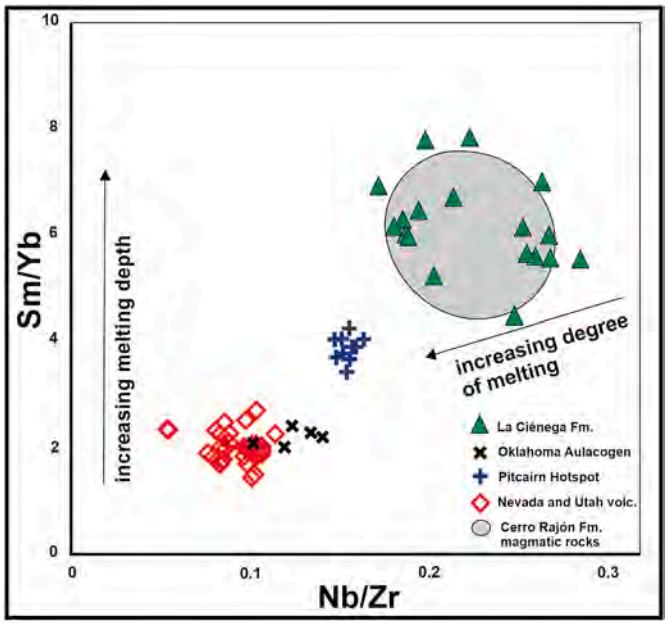

Fig. 9. Trace element diagram that describes relative mantle melting rates and melting depth for La Ciénega Formation subvolcanic metabasalts and potentially contemporaneous rift and hotspot basaltic rocks. Data includes the La Ciénega Formation and contemporaneous volcanic rocks from Nevada and Utah (Stirling Quartzite, Wood Canyon Formation, Prospect Mountain Quartzite, Tintic Quartzite, Browns Hole Formation; Hagadorn and Holm-Denoma, 2016), Southern Oklahoma Aulacogen (Brueseke et al., 2016) and Pitcairn Island volcanics (Garapić et al., 2015), and Cerro Raón Formation (Barrón-Díaz et al., 2019a). After He et al. (2010).

Relatively low ratios of partial melting are observed in the metabasalts from La Ciénega Formation (Fig. 9) (He et al., 2010), when compared to contemporaneous rift basalts with E-MORB characteristics from Nevada and Utah (Barrón-Díaz et al., 2022) and the Southern Oklahoma Aulacogen tholeiitic basalts (Brueseke et al., 2016) and volcanics from the Pitcairn Island hot spot that have EMI signatures (Garapić et al., 2015). In contrast, the inferred mantle melting rates and melting depths for La Ciénega volcanic rocks overlap those calculated from Sm/Yb and Nb/Zr ratios from the overlying Cerro Rajón Formation volcanic rocks (Barrón-Díaz et al., 2019a). These major and trace element analyses, together with immobile trace element and radiogenic data suggest the La Ciénega sills are geochemically indistinguishable from the Cerro Rajón Formation flows. Given this context, the origin of the La Ciénega metabasalts is best explained that they were emplaced by the conduits that brought the magma to the surface during deposition of the Cerro Rajón Formation volcanics (Fig. 10).

6. Conclusions and future directions

Field relationships and petrologic aspects of the La Ciénega Formation mafic-ultramafic rocks suggest they are intrusive sills that were emplaced as shallow subvolcanic bodies. Their mineralogy and textures record extensive actinolite-chlorite-albite and clay-carbonate alteration of original basaltic rocks. The sequence is affected by greenschist facies contact metamorphism. Immobile trace and major elements suggest the alkali basalt protolith was derived from ultrabasic alkaline magmatism.

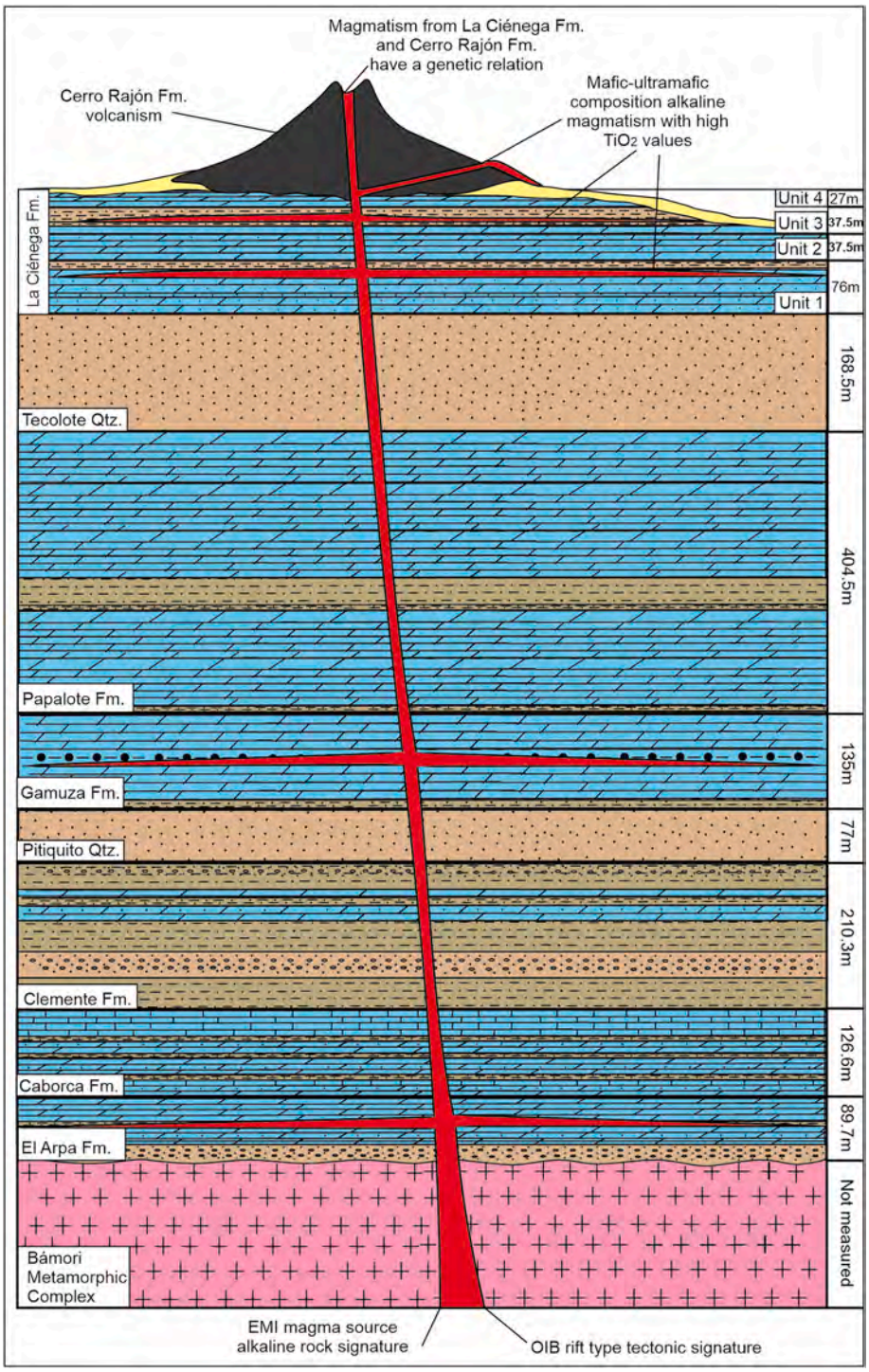

Fig. 10. Hypothesized genetic scheme of La Ciénega Formation magmatism. This illustrates a mechanism to account for the mafic intrusions in the La Ciénega, Gamuza, and El Arpa Formations that ties them to the overlying Cerro Rajón Formation. Section thickness adapted from Stewart et al. (1984). Volcano is for illustrative purposes only. It is not to scale.

Trace element, REE, and tectonic discrimination diagrams relate these volcanic rocks to a continental intraplate domain characterized by magmas that may have ascended by adiabatic decompression into a rift zone. Isotopic data relates the La Ciénega Formation metabasalts to an EMI mantle source, but the high $^{87}Sr/^{86}Sr$ content in these rocks could result from crustal assimilation and mixing during magmatic ascent—a characteristic consistent with continental rifting. La Ciénega Formation sills have similar geochemical characteristics to the overlying Cerro Rajón Formation flows and stratigraphically lower El Arpa Formation sill, suggesting near-contemporaneous emplacement (see Fig. 10) in a Cambrian continental rift that developed along southern Laurentia (Hammond, 1984; Colpron et al., 2002; Yonkee et al., 2014). Further geochemical and isotopic studies in volcanic rocks of comparable age in western North America are required to determine the geodynamic evolution of this system and how widespread this magmatic event or suite of events was along the western Laurentian margin. These results are a first step toward such continental margin-scale petrogenetic studies and provide a comparison point for future studies of

contemporaneous volcanism.

Declaration of competing interest

The authors declare that they have no known competing financial interest or personal relationships that could have appeared to influence the work reported in this paper.

Acknowledgements

We are grateful to the patrons of the DMNS Earth Science Department for supporting analytical costs for this project. We thank R. Lizarraga and all the landowners who allowed us to conduct fieldwork on their land and O. Navarro and the team at Fresnillo for accommodations during field work. S. Corral and J. Chang are thanked for preparation of thin sections. We thank three anonymous reviewers for their comments which helped to improve this manuscript. Any use of trade, product, or firm names in this publication is for descriptive purposes only and does not imply endorsement by the U.S. government.

Appendix A. Supplementary data

Supplementary data to this article can be found online at https://doi.org/10.1016/j.apgeochem.2022.105375.

References

Barrón-Díaz, A.J., 2019. Petrogénesis y metamorfismo del magmatismo Cámbrico de la Formación Cerro Rajón, Sonora, México y su relación con el proceso de rifting en el margen meridional de Laurentia. In: Universidad Nacional Autónoma De México Programa de posgrado en ciencias de la tierra instituto de geología estación regional del noroeste, Tesis doctoral, Hermosillo. Sonora, México.

Barrón-Díaz, A.J., 2013. Caracterización petrogenética de las metabasitas anorogénicas del límite Cámbrico-Precámbrico, Municipio de Pitiquito, Sonora, México [M.S. thesis]. Universidad de Sonora, p. 95.

Barrón-Díaz, A.J., Paz-Moreno, F.A., Lozano-Santa Cruz, R., Herrera-Urbina, S., Centeno-García, E., López-Martínez, M., 2019a. Early Cambrian alkaline volcanism on the southern margin of Laurentia: evidence in the volcaniclastic units from the Puerto Blanco Formation in the Caborca block, NW Mexico. Int. Geol. Rev. 61 (10), 1189–1206.

Barrón-Díaz, A.J., Hagadorn, J., Paz-Moreno, F.A., Martínez-Valencia, D., Holm-Denoma, C., 2022. Ediacaran-Cambrian rift related volcanism in western Laurentia Aborted rift event(s)? Geol. Soc. Am. Abstr. Progr. 54 (2).

Barrón-Díaz, A.J., Paz-Moreno, F.A., Hagadorn, J.W., 2019b. The Cerro Rajón Formation—a new lithostratigraphic unit proposed for a Cambrian (Terreneuvian) volcano-sedimentary succession from the Caborca region, northwest Mexico. J. S. Am. Earth Sci. 89, 197–210.

Barrón-Díaz, A.J., Paz-Moreno, F.A., Miggins, D.P., Iriondo, A., 2019c. Geochronology and geothermometry of the laramidic metamorphism in the Cambrian metabasalts from the Cerro Rajón Formation, Caborca region, northwest Mexico. J. S. Am. Earth Sci. 41, 45–56.

Bond, G.C., Christie-Blick, N., Kominz, M.A., Devlin, W.J., 1985. An early Cambrian rift to post-rift transition in the Cordillera of western North America. Nature 114, 742–745.

Brueseke, M.E., Hobbs, J.M., Bulen, C.L., Mertzman, S.A., Puckett, R.E., Walker, J.D., Feldman, J., 2016. Cambrian intermediate-mafic magmatism along the Laurentian margin: evidence for flood basalt volcanism from well cuttings in the Southern Oklahoma Aulacogen. U.S.A.), Lithos 260, 164–177.

Cabanis, B., Lecolle, M., 1989. Le diagramme La/10-Y/15-Nb/8: un outil pour la discrimination des séries volcaniques et la mise en évidence des processus de mélange et/ou de contamination crustale. Comptes rendus de l'Académie des sciences. Série 2, Mécanique, Physique, Chimie, Sciences de l'univers, Sciences de la Terre 309 (20), 2023–2029.

Callegari, E., Pertsev, N.N., 2007. Contact metamorphic rocks. In: Recommendations by the IUGS Subcommission on the Systematics of Metamorphic Rocks. www.bgs.ac.uk/scmr/home.html.Web version, 1, 2007.

Centeno-García, E., Maytorena, F., Calmus, T., Solis-Pichardo, G., Lozano-Santa Cruz, R., 2002. Proterozoic OIB magmatism in the Caborca terrane, northwestern Mexico. In: Denver Annual Meeting. Colorado Convention Center: C205. Session No. 245.

Crittenden Jr., M.D., Schaeffer, F.E., Trimble, D.E., Woodward, L.A., 1971. Nomenclature and correlation of some upper Precambrian and basal Cambrian sequences in western Utah and southeastern Idaho. Geol. Soc. Am. Bull. 82 (3), 581–602.

Colpron, M., Logan, J.M., Mortensen, J.K., 2002. U-Pb zircon age constraint for late Neoproterozoic rifting and initiation of the lower Paleozoic passive margin of western Laurentia. Can. J. Earth Sci. 39 (2), 133–143.

Eells, J.L., 1972. Geology of the Sierra de La Berruga, north-western Sonora, Mexico [M. S. thesis. San Diego. California State University, p. 77.

Garapić, G., Jackson, M.G., Hauri, E.H., Hart, S.R., Farley, K.A., Blusztajn, J.S., Woodhead, J.D., 2015. A radiogenic isotopic (He-Sr-Nd-Pb-Os) study of lavas from the Pitcairn hotspot: implications for the origin of EM-1 (enriched mantle 1). Lithos 228–229, 1–11.

Hagadorn, J.W., Holm-Denoma, C.S., 2016. Linking Neoproterozoic to Cambrian strata from Sonora to Utah. In: Geological Society of America Abstracts with Programs, vol. 48. No. 7.

Hammond, J.L.G., 1984. Late Precambrian diabase intrusions in the southern death valley region. In: California: Their Petrology, Geochemistry, and Tectonic Significance. M.S. Thesis, University of Southern California, p. 295.

He, Q., Xiao, L., Balta, B., Gao, R., Chen, J., 2010. Variety and complexity of the late–Permian Emeishan basalts: Reappraisal of plume–lithosphere interaction processes. Lithos 119, 91–107. https://doi.org/10.1016/j.lithos.2010.07.020.

Hodgin, E.B., Nelson, L.L., Wall, C.J., Barron-Diaz, A.J., Webb, L.C., Schmitz, M.D., Fike, D.A., Hagadorn, J.W., Smith, E.F., 2021. A link between rift-related volcanism and end-Ediacaran extinction? Integrated chemostratigraphy, biostratigraphy, and U-Pb geochronology from Sonora. Mexico: Geology 49, 115–119.

Hoernle, K., Hauff, F., Werner, R., van den Bogaard, P., Gibbons, A.D., Conrad, S., Muller, R.D., 2011. Origin of Indian Ocean Seamount Province by shallow recycling of continental lithosphere. Nat. Geosci. 4, 883–887. https://doi.org/10.1038/ngeo1331.

Kimura, J.I., Gill, J.B., Skora, S., van Keken, P.E., Kawabata, H., 2016. Origin of geochemical mantle components: Role of subduction filter. G-cubed 17 (8), 3289–3325.

Loyd, S.J., Marenco, P.J., Hagadorn, J.W., Lyons, T.W., Kaufman, A.J., Sour-Tovar, F., Corsetti, F.A., 2012. Sustained low marine sulfate concentrations from the Neoproterozoic to the Cambrian: insights from carbonates of northwestern Mexico and eastern California. Earth Planet Sci. Lett. 339–340, 79–94.

Loyd, S.J., Marenco, P.J., Hagadorn, J.W., Lyons, T.W., Kaufman, A.J., Sour-Tovar, F., Corsetti, F.A., 2012. Local δ34S variability in ~580 Ma carbonates of northwestern Mexico and the Neoproterozoic marine sulfate reservoir. Precambrian Res. 224, 551–569.

Loyd, S.J., Marenco, P.J., Hagadorn, J.W., Lyons, T.W., Kaufman, A.J., Sour-Tovar, F., Corsetti, F.A., 2012. Sustained low sulfate concentrations in the Neoproterozoic to Cambrian ocean: insights from carbonates of northwestern Mexico and eastern California. Earth Planet Sci. Lett. 339–340, 79–94.

Lund, K., Aleinikoff, J., Evans, K., Dewitt, E., Unruh, D., 2010. SHRIMP U–Pb dating of recurrent Cryogenian and Late Cambrian–Early Ordovician alkalic magmatism in central Idaho: implications for Rodinian rift tectonics. Geol. Soc. Am. Bull. 122, 430–453.

Pearce, J.A., 1996. A user's guide to basalt discrimination diagrams. Trace element geochemistry of volcanic rocks: applications for massive sulphide exploration. Geological Association of Canada, Short Course Notes 12 (79), 113.

Pearce, J.A., 2008. Geochemical fingerprinting of oceanic basalts with applications to ophiolite classification and the search for Archean oceanic crust. Lithos 100 (1–4), 14–48.

Shervais, J.W., 2022. The petrogenesis of modern and ophiolitic lavas reconsidered: Ti-V and Nb-Th. Geosci. Front. 13 (2), 101319.

Sour-Tovar, F., Hagadorn, J.W., Huitrón-Rubio, T., 2007. Ediacaran and Cambrian index fossils from Sonora, Mexico. Paleontology 50 (1), 169–175.

Stewart, J.H., 1972. Initial Deposits of the Cordilleran Geosyncline: Evidence of a Late Precambrian (850 m.y.) Continental Separation, vol. 83. Geological Society of America Bulletin, pp. 1345–1360.

Stewart, J.H., McMenamin, A.S., Morales-Ramirez, J.M., 1984. Upper Proterozoic and Cambrian rocks in the Caborca region, Sonora, Mexico. In: Physical Stratigraphy, Biostratigraphy, Paleocurrents Studies and Regional Relations. U. S. Geological Survey Professional. Paper 1390.

Stewart, J.H., 1991. Latest Proterozoic and Cambrian rocks of the western United States— an overview. In: Cooper, J.D., Stevens, C.H. (Eds.), Paleozoic Paleogeography of the Western United States-II, Volume 1. Los Angeles, Pacific Section, vol. 67. Society of Economic Paleontologists and Mineralogists, Book, pp. 13–38.

Stewart, J.H., Amaya-Martinez, R., Palmer, A.R., 2002. In: Neoproterozoic and Cambrian Strata of Sonora, Mexico: Rodinian Supercontinent to Laurentian Cordilleran Margin, vol. 365. Geológical Society of América, Special Paper, pp. 5–48.

Stracke, A., Bizimis, M., Salters, V.J., 2003. Recycling oceanic crust: quantitative constraints. G-cubed 4 (3).

Stracke, A., Hofmann, A.W., Hart, S.R., 2005. FOZO, HIMU, and the rest of the mantle zoo. G-cubed 6 (5).

Sun, S.S., McDonough, W.F., 1989. Chemical and isotopic systematics of oceanic basalts: implications for mantle composition and processes. Geological Society, London, Special Publications 42 (1), 313–345.

Tappe, S., Foley, S.F., Stracke, A., Romer, R.L., Kjarsgaard, B.A., Heaman, L.M., Joyce, N., 2007. Craton reactivation on the Labrador Sea margins: 40Ar/39Ar age and Sr–Nd–Hf–Pb isotope constraints from alkaline and carbonatite intrusives. Earth Planet Sci. Lett. 256 (3–4), 433–454.

Tatsumoto, M., Nakamura, Y., 1991. DUPAL anomaly in the Sea of Japan: Pb, Nd, and Sr isotopic variations at the eastern Eurasian continental margin. Geochem. Cosmochim. Acta 55 (12), 3697–3708. https://doi.org/10.1016/0016-7037(91)90068-G.

Willbold, M., Stracke, A., 2006. Trace element composition of mantle end-members: implications for recycling of oceanic and upper and lower continental crust. Geochem. Geophys. Geosyst. 7, Q04004 https://doi.org/10.1029/2005GC001005.

Willbold, M., Stracke, A., 2010. Formation of enriched mantle components by recycling of upper and lower continental crust. Chem. Geol. 276 (3–4), 188–197. https://doi.org/10.1016/j.chemgeo.2010.06.005.

Wood, D.A., 1980. The application of a Th-Hf-Ta diagram to problems of tectonomagmatic classification and to establishing the nature of crustal contamination of basaltic lavas of the British Tertiary Volcanic Province. Earth Planet Sci. Lett. 50 (1), 11–30.
Yonkee, W.A., Dehler, C.D., Link, P.K., Balgord, E.A., Keeley, J.A., Hayes, D.S., Wells, M. L., Fanning, C.M., Johnston, S.M., 2014. Tectono-stratigraphic framework of Neoproterozoic to Cambrian strata, west-central US: Protracted rifting, glaciation, and evolution of the North American Cordilleran margin. Earth Sci. Rev. 136, 59–95.
Zindler, A., Hart, S.R., 1986. Chemical geodynamics. Annu. Rev. Earth Planet Sci. 14 (1), 493–571. https://doi.org/10.1146/annurev.ea.14.050186.002425.